Pergamon

Cement and Concrete Research, Vol. 28, No. 12, pp. 1725–1736, 1998

0008-8846/98 $–see front matter

PII S0008-8846(98)00157-4

SIZE EFFECT ON FLEXURAL, SPLITTING TENSILE, AND TORSIONAL STRENGTHS OF HIGH-STRENGTH CONCRETE

F.P. Zhou,[1] R.V. Balendran, and A.P. Jeary
Department of Building and Construction, City University of Hong Kong, Hong Kong

(Received January 28, 1998; in final form September 9, 1998)

ABSTRACT

This paper presents the results of an investigation into the size effect on flexural, splitting tensile, and torsional strengths of high-strength concrete (HSC) with normal aggregate (crushed limestone) and lightweight aggregate (sintered fly ash). The Bazant's size effect law gives a very good fit to the flexural strengths of both normal and lightweight aggregate HSC measured from beams of different sizes. As observed in the size effect curve, the fracture behavior of the lightweight HSC seems more brittle than that of the normal HSC. Linear elastic fracture mechanics may still be less applicable to HSC in the normal size range than nonlinear fracture mechanics. A reverse size effect is observed in the prism splitting tensile strengths of both normal and lightweight HSC and possible mechanisms of the reverse size effect are discussed. The torsional strength of the lightweight HSC appears to have a stronger size dependency than that of the normal HSC. © *1998 Elsevier Science Ltd*

Introduction

It is well known that strengths of concrete structures exhibit some size dependency; strengths of geometrically similar structures decrease with increasing size (1). Intensive studies on the fracture of concrete in the last two decades have clarified that the size effect on strength is related primarily to a relatively large fracture propagation process (FPZ) in concrete (2). Nonlinear fracture models, i.e., the Fictitious Crack Model by Hillerborg et al. (3), the Crack Band Model by Bazant and Oh (4), and the Two-Parameter Model by Jenq and Shah (5), have been applied to the analysis and prediction of size effects in concrete structures (2,6,7). The size effect law proposed by Bazant (8), although simple, can describe satisfactorily the size dependency of flexural strength (8), splitting tensile strength (9), and torsional strength (10,11).

With the advance in concrete technology, high-strength concrete (HSC) with normal and lightweight aggregates has been increasingly used in buildings and civil engineering structures and has received enormous research attention (12). Although HSC tends to be more brittle (13–15) with increasing strength, the research on the fracture behavior of HSC has been limited. It is felt that the study of the size effect in HSC may help to understand the

[1]To whom correspondence should be addressed.

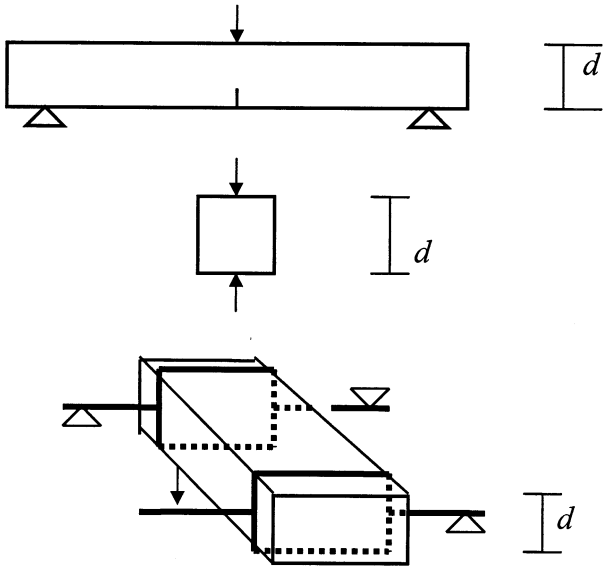

FIG. 1.
Schematic illustrations of flexural, splitting, and torsional tests.

behavior of HSC and predict load-bearing capacities of different types and sizes of HSC structures. Therefore, an experimental study was carried out to examine the size effect on flexural, splitting tensile, and torsional strengths of HSC with normal and lightweight aggregates.

Experimental Details

Test methods

The influence of specimen size on flexural, splitting tensile, and torsional strengths was investigated by conducting three-point bending, splitting, and torsional tests, respectively, on specimens of different sizes (Fig. 1). The test types and specimen sizes are shown in Table 1. The cube compressive and cylinder splitting strengths were determined in accordance with BS1881: Parts 116 and 117, respectively.

In the three-point bending tests, the crack mouth opening displacement (CMOD), measured by means of a CMOD gauge, was used as the feedback control variable to ensure stable tests. The deflection was measured by an LVDT transducer. The load–deflection and load–CMOD curves were recorded for the evaluation of flexural strength and fracture properties. The splitting tensile tests were conducted by load control and only the ultimate loads were recorded. The torsional tests were performed by displacement control, and load–displacement curves were recorded.

TABLE 1
Test type and specimen size.

Test type	Dimensions (mm)	Properties
Cube compression	100 × 100 × 100	Compressive strength
Cylinder splitting	ϕ 100 × 200	Tensile strength
Three-point bending	50 × 100 × 200 × 300*	Flexural strength
	100 × 100 × 400 × 500*	
	200 × 100 × 800 × 840*	
Prism splitting	76 × 76 × 100	
	100 × 100 × 100	Tensile strength
	100 × 100 × 100	
	150 × 150 × 100	
	200 × 200 × 100	
Torsion	50 × 100 × 200	Torsional strength
	100 × 200 × 400	

* Height, width, span and length of beams.

Mix proportions and specimen preparation

The mix proportions of the two types of HSC are given in Table 2 and the volume fractions of cement, silica fume, water, sand, and coarse aggregate were the same. The water-to-binder (cement + silica fume) ratio was 0.28 and the silica fume replacement [S/(C+S)] was 10%. The superplasticizer used was Conplast 430 of sulfated naphthalene formaldehyde condensate type and the amount was about 1% by weight of the binder content. The silica fume was in the form of slurry at 50% concentration. The normal aggregate of crushed limestone had a maximum size of 10 mm and an oven-dry density of 2640 kg/m^3, whereas the lightweight aggregate of sintered fly ash had a maximum size of 6 mm and an oven-dry density of 1520 kg/m^3.

In mixing, the cement, sand, and coarse aggregates were normally blended first and the silica fume, superplasticizer, and water were then added. In the case of the lightweight concrete, the lightweight aggregate was first mixed with enough water for the short-term

TABLE 2
Concrete mix proportions.

Material	Normal HSC (kg/m^3)	Lightweight HSC (kg/m^3)
Cement	440	440
Silica fume	49	49
Water (free)	136	136
Sand	660	660
Limestone	1105	0
Sintered fly ash	0	636

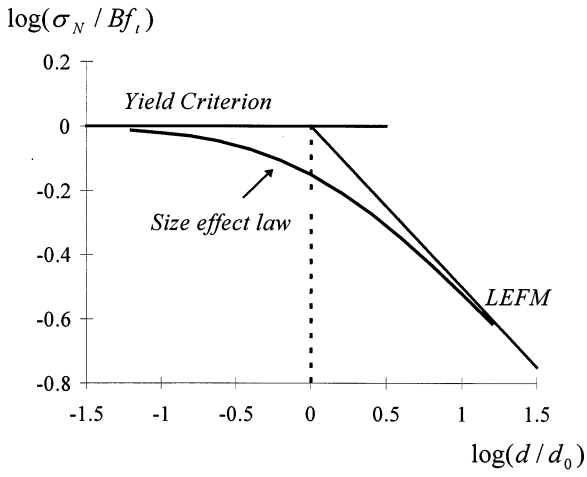

FIG. 2.
Size effect law proposed by Bazant (8).

absorption for half an hour before blending with cement and sand. The specimens were demolded after 1 day and stored in a water tank at 20°C for about 90 days. Notches in beams were introduced by a diamond saw 1 day before testing.

Theoretical Background

The size dependency of nominal strength of geometrically similar concrete structures may be described by the size effect law proposed by Bazant (8) (Fig. 2):

$$\sigma_N = \frac{Bf_t}{\sqrt{1+\beta}} \quad \beta = \frac{d}{d_0} \tag{1}$$

where f_t is the material tensile strength, β is the brittleness number, and B and d_0 are empirical constants. The nominal strength of two-dimensional similar structures is defined as (Eq. 2):

$$\sigma_N = c_n \frac{P_u}{bd} \tag{2}$$

where c_n is a coefficient introduced for convenience, P_u is the ultimate load, b is the specimen thickness, and d is the characteristic specimen size (i.e., height of the beam). When β is very small (e.g., <0.1), the behavior of a structure is more ductile and the nominal strength of the structure approaches the plastic or yield limit. But when β is very large (e.g., >10), the behavior tends to be more brittle and the nominal strength approaches the prediction by linear elastic fracture mechanics (LEFM).

To facilitate the evaluation of the constants in the size effect law, Eq. 1 can be transformed into Eq. 3:

TABLE 3
Basic material properties.

Concrete	Density (kg/m^3)	Compressive strength (MPa)	Splitting tensile strength (MPa)	Dynamic modulus of elasticity (GPa)
Normal HSC	2430	115	4.50	49
Lightweight HSC	2013	90	3.33	29

$$\left(\frac{f_t}{\sigma_N}\right)^2 = \frac{1}{d_0 B^2}\, d + \frac{1}{B^2}. \tag{3}$$

If the experimental data are arranged in a plot of $X = d$ and $Y = (f_t/\sigma_N)^2$, a linear regression equation may be found as $Y = AX + C$. B and d_0 can be evaluated from A and C as (Eq. 4):

$$B = 1/\sqrt{C}, \quad d_0 = C/A. \tag{4}$$

The size range should be sufficiently large (at least 1:4) and at least three sizes should be used.

Results and Discussion

Basic properties

The basic properties of the HSC with normal aggregate (crushed limestone) and lightweight aggregate (sintered fly ash) are given in Table 3. The replacement of the normal aggregate in HSC with the lightweight aggregate results in a 22% reduction in the compressive strength, a 26% reduction in the splitting tensile strength, and a 41% reduction in the dynamic modulus of elasticity. In other words, the use of lightweight aggregate in HSC causes a higher reduction in the splitting tensile strength and dynamic modulus of elasticity than in the compressive strength. The ratios of splitting tensile strength to compressive strength are 3.9% and 3.7% for the normal and lightweight HSC, respectively, and are much lower than the typical value of 8–15% for normal strength concrete. Therefore, HSC may have a relatively lower resistance to cracking than normal strength concrete.

Flexural strength

The nominal flexural strength of a notched beam subjected to three-point bending was calculated from the following expression (Eq. 5):

$$\sigma_N = \frac{3PS}{2bd^2} \tag{5}$$

where P is the ultimate load, and S, b, and d are the span, thickness, and height of the beam, respectively. The notch ratio (a/d) was 1/3 and the span/height ratio (S/d) was 4. The mean

TABLE 4
Flexural strength measured from notched beams of three sizes.

Concrete	Flexural strength (MPa)		
	d = 50 (mm)	d = 100 (mm)	d = 200 (mm)
Normal HSC	3.43	2.74	2.19
Lightweight HSC	2.28	1.52	1.20

nominal flexural strengths of the two types of HSC measured from different sizes of beams are shown in Table 4 and the experimental data are plotted in Figure 3. The flexural strengths of both types of HSC decrease as the specimen size increases, which is similar to the trend observed in normal strength concrete (3,8). But a stronger size effect on flexural strength is found in the lightweight HSC than in the normal HSC. When the beam size increases from 50 to 100 mm, and from 100 to 200 mm, the decrease in flexural strength is 33% and 21%, respectively, for the lightweight HSC but is 20% in both cases for the normal HSC. The flexural strength values of the lightweight HSC measured from 50-, 100-, and 200-mm high beams are about 66%, 56%, and 55% of the corresponding values of the normal HSC.

In other words, the use of the lightweight HSC can cause a higher reduction in the load-carrying capacity of a larger structure than of a small structure.

In order to evaluate the size effect law, the experimental data were rearranged in a plot of $X = d$ and $Y = (f_t/\sigma_N)^2$ in Figure 4. The cylinder splitting tensile strengths in Table 2 were used as the material tensile strengths (f_t). The linear regression equations of $X = d$ and $Y = (f_t/\sigma_N)^2$ derived for both types of HSC are given in Figure 4. For the normal aggregate HSC, the slope and the intercept of the linear regression equation are $A = 0.0167$ and $C = 0.9767$, respectively. Therefore, the two constants in the size effect law can be calculated as $B =$

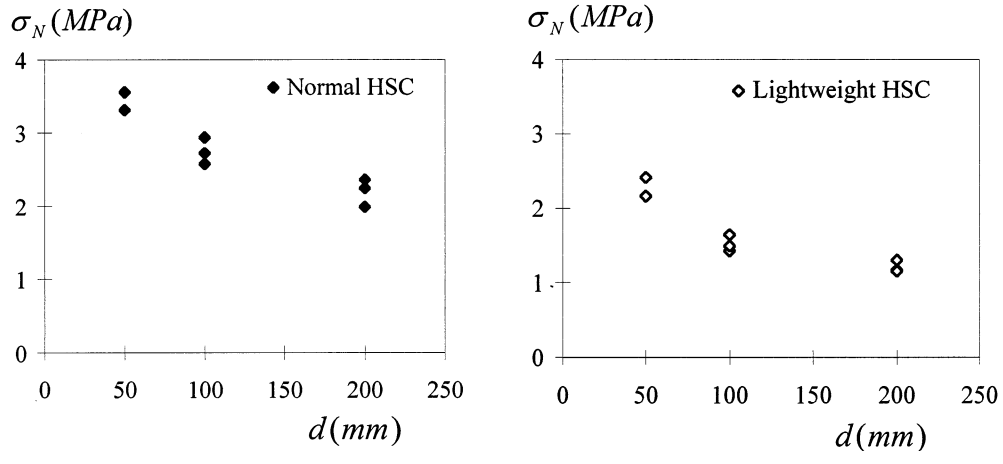

FIG. 3.
Influence of beam size on nominal flexural strength.

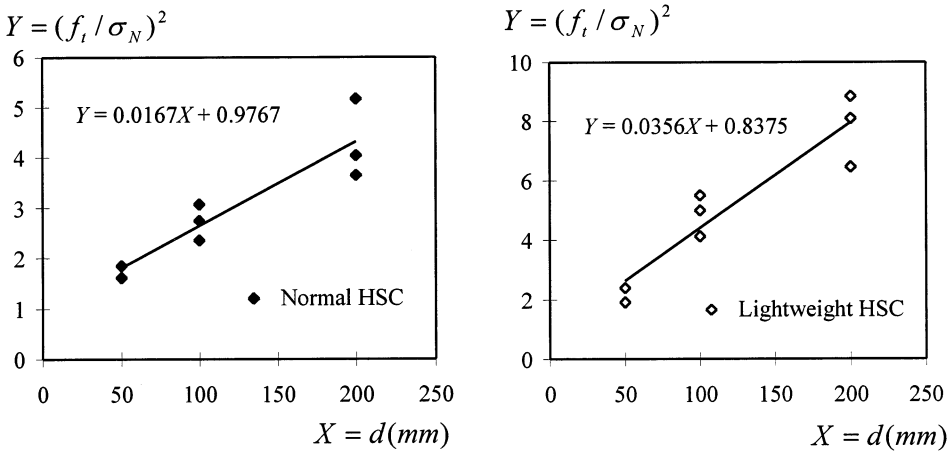

FIG. 4.
Linear regression for determining constants in size effect law.

$1/\sqrt{C} = 1.012$ and $d_0 = C/A = 58.5$ (mm). The size effect law for the normal HSC can be expressed as (Eq. 6):

$$\sigma_N = \frac{1.012 f_t}{\sqrt{1 + 0.017d}}. \tag{6}$$

For the lightweight HSC, the slope and the intercept are $A = 0.0356$ and $C = 0.8375$, respectively. Therefore, $B = 1/\sqrt{C} = 1.093$ and $d_0 = C/A = 23.5$ (mm). The size effect law for the lightweight HSC can be expressed as (Eq. 7):

$$\sigma_N = \frac{1.093 f_t}{\sqrt{1 + 0.042d}}. \tag{7}$$

The experimental data of the normal and lightweight aggregate HSC are compared in Figure 5 on a double logarithmic scale of σ_N/Bf_t and d/d_0 and the Bazant's size effect law fits the experimental data very well. Clearly, the data points of the lightweight HSC shift more towards the prediction by LEFM than those of the normal HSC, which suggests a more brittle behavior in the lightweight HSC than in the normal HSC. However, LEFM may still be less applicable to HSC than nonlinear fracture mechanics as β is <10 in the normal size range.

Splitting tensile strength

In the splitting tests on prismatic specimens, the tensile strength was evaluated from Eq. 8:

$$f_{SP} = \frac{2P}{\pi dl} \tag{8}$$

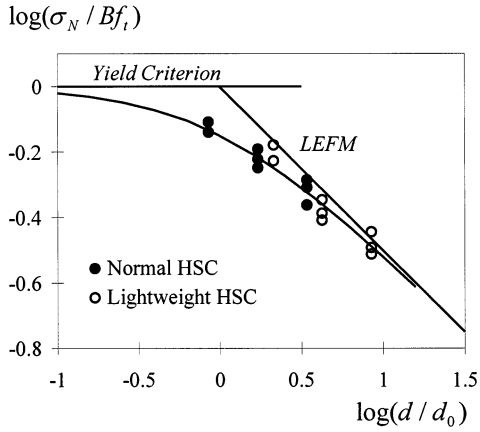

FIG. 5.
Size effect law of flexural strength.

where P is the ultimate load, and d and l are the height and length of specimens, respectively. The mean tensile strength values are given in Table 5 and the experimental data are plotted in Figure 6. As can be seen in Table 5 and Figure 6, the splitting tensile strengths of both types of HSC exhibit a reverse size effect, i.e., tensile strength increases with increasing size. That is contrary to the normal size effect: strength decreasing with increasing size. The lightweight HSC indicates a stronger reverse size effect than the normal HSC. A similar reverse size effect also has been reported in the splitting tests on cylinders of normal strength concrete by Bazant et al. (9) and Hasegawa et al. (16). As the specimen size increased, the splitting tensile strength first decreased in the small size range, then increased gradually in the intermediate size range, and finally approached a constant value in the large size range. Bazant et al. (9) explained it as a result of the interaction of two failure mechanisms: wedge slip and axial splitting.

Tang et al. (17) conducted a theoretical analysis of cylinder splitting tests employing the Two-Parameter Model (5) and finite element method. They found that the contact width between the loading platen and cylinder in a splitting test had a great influence on the size effect curve. When the width was small (3 mm), a reverse size effect curve was predicted.

TABLE 5
Splitting tensile strength measured from prisms of different sizes.

	Splitting tensile strength (MPa)			
Concrete	76 × 76 × 100 (mm)	100 × 100 × 100 (mm)	150 × 150 × 100 (mm)	200 × 200 × 100 (mm)
Normal HSC	4.15	5.37	5.89	5.80
Lightweight HSC	3.57	2.96	3.94	4.64

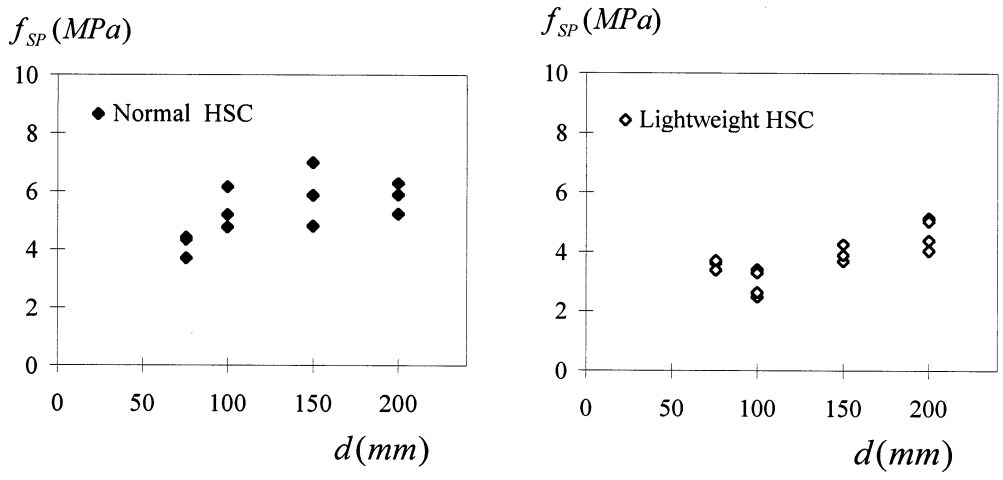

FIG. 6.
Influence of prism size on splitting tensile strength.

But when the width was large (15 mm), a normal size effect curve was produced. The size effect curves for different widths differ mainly in the small size range but are identical in the large size range.

As the width is related to the size of the wedge slip zone, it may be inferred that the wedge slip plays a major role in the observed reverse size effect. Conceivably, the wedge slip may have a more important influence on the failure process in small specimens than in large specimens, as the ratio of the size of the wedge slip zone to the specimen size decreases with increasing specimen size. A small wedge zone may imply a low slip force and result in a low ultimate failure load in small specimens if the wedge slip dominates the failure. However, the axial force may be considerably greater than the wedge slip force in large specimens so that the ultimate failure load and the measured splitting strength may not be affected significantly by the contact width.

On the other hand, if two different materials are tested with the same contact width between the loading platen and specimen, the wedge slip force in the weaker material may be lower than that in the stronger material, which may have the same effect as a smaller contact width. Therefore, a stronger reverse size effect may be expected in the weaker material, which may explain the different size effects observed in the two types of HSC in the present study.

The splitting test is believed to give a closer representative value of the true tensile strength of concrete. However, if a strong reverse size effect occurs, the splitting strength measured from small specimens may be lower than the true strength. Actually, it has been suggested that the splitting tests might yield too low a value of tensile strength in the case of lightweight aggregate concrete of normal strength (18). As the splitting test is very important for the measurement of tensile strength of concrete, it is necessary to carry out a further numerical study to clarify the interaction of different failure mechanisms in splitting tests.

TABLE 6
Torsional strength measured from prisms of different sizes.

Concrete	Torsional strength (MPa)	
	50 × 100 × 200 (mm)	100 × 200 × 400 (mm)
Normal HSC	5.63	5.30
Lightweight HSC	4.09	2.93

Torsional strength

The torsional strength measured from torsional tests on beams of a rectangular cross-section was calculated using Eq. 9:

$$v_N = \frac{T}{\alpha b d^2} \tag{9}$$

where T is the ultimate torque, b and d are the width and height of beams ($b \geq d$), and α is a constant depending on the ratio b/d. When $b/d = 2$, $\alpha = 0.246$. The mean torsional strengths of the normal and lightweight aggregate HSC are shown in Table 6 and the experimental data are plotted in Figure 7.

Because of the limit of the set-ups, only two sizes of beams were tested and are not enough for the evaluation of the size effect law. But some trend in the influence of specimen size on torsional strength may still be observed. As can be seen in Table 6 and Figure 7, the torsional strength of the lightweight HSC seems more size dependent than that of the normal HSC. When the specimen size (d) increases from 50 to 100 mm, the mean torsional strength

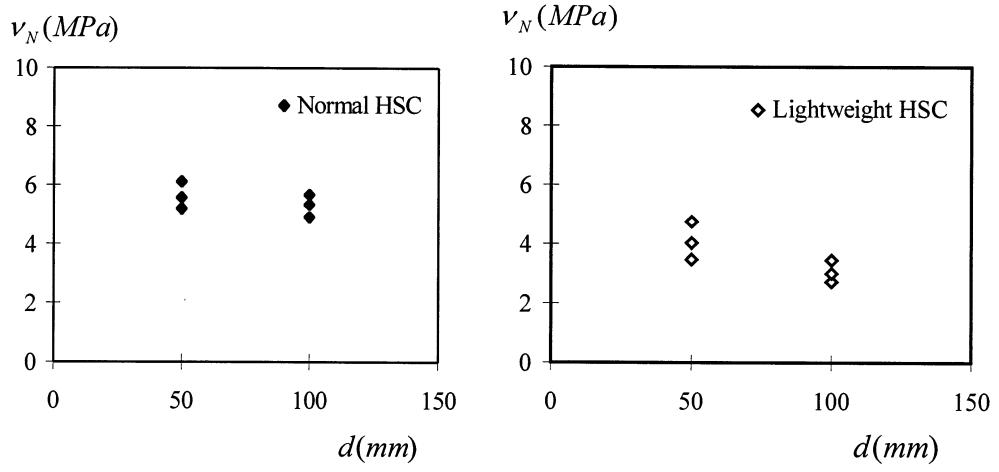

FIG. 7.
Influence of prism size on torsional strength.

decreases only 5% for the normal HSC but 28% for the lightweight HSC. The torsional strength of the lightweight HSC is about 27% lower than that of the normal HSC when measured from the small beam, whereas it is 45% lower when measured from the larger beam. Special attention may need to be paid to the considerably low torsional strength of lightweight HSC in the design of larger structures.

Conclusions

An experimental study has been conducted to investigate the size effect on flexural, splitting tensile, and torsional strengths of HSC with normal aggregate (crushed limestone) and lightweight aggregate (sintered fly ash). The following conclusions may be drawn.

1. The Bazant's size effect law gives a very good account of the size dependency of flexural strength for both normal and lightweight HSC. As observed in the size effect curve, the fracture behavior of the lightweight HSC seems to be more brittle than that of the normal HSC. LEFM may still be less applicable to HSC in the normal size range than nonlinear fracture mechanics.
2. A reverse size effect has been observed in the prism splitting tensile strengths of both normal and lightweight HSC. The reverse size effect observed in the lightweight HSC is stronger than in the normal HSC. The splitting tensile strength measured on the standard size might yield too low a value of the true strength for the lightweight HSC. The possible mechanisms of the reverse size effect have been discussed and a further numerical study may be required.
3. The torsional strength of the lightweight HSC appears to have a stronger size dependency than that of the normal HSC. The use of lightweight HSC instead of normal HSC may result in a higher reduction in the torsional strength of large beams than in that of small beams.

References

1. H. Mihashi, H. Okamura and Z.P. Bazant (eds.) Size Effect in Concrete Structures, E & FN Spon, London, 1994.
2. S.P. Shah, S.E. Swartz and C. Ouyang, p. 552, Fracture Mechanics of Concrete, John Wiley & Sons, Inc., New York, 1995.
3. A. Hillerborg, M. Modeer and P.E. Petersson, Cem. Concr. Res. 6, 773 (1976).
4. Z.P. Bazant and B.H. Oh, Mater. Struct. 16, 155 (1983).
5. Y.S. Jenq and S.P. Shah, J. Eng. Mech. 111, 1227 (1985).
6. A. Carpinteri, Applications of Fracture Mechanics to Reinforced Concrete, Elsevier Science Publishers Ltd., England, 1992.
7. P.J. Gustafsson and A. Hillerborg, ACI Struct. J. 85, 286 (1988).
8. Z.P. Bazant, J. Engrg. Mech. 110, 518 (1985).
9. Z.P. Bazant, M.T. Kazemi, T. Hasegawa, and J. Mazars, ACI Mater. J. 88, 325 (1991).
10. Z.P. Bazant, S. Sener and P. Prat, Mater. Struct. 21, 425 (1988).
11. B. Barr and Z.Y. Tokatly, Applications of Fracture Mechanics to Reinforced Concrete, A. Capinteri (ed.), Elsevier Science Publishers Ltd., England, 1992.
12. S.P. Shah and S.H. Agmad, High Performance Concrete: Properties and Applications, p. 403, McGraw-Hill, Inc., New York, 1994.
13. R. Gettu, Z.P. Bazant and M.E. Karr, ACI Mater. J. 87, 608 (1990).

14. F.P. Zhou, B. Barr and F.D. Lydon, Cem. Concr. Res. 25, 543 (1995).
15. M.-H. Zhang and O.E. Gjorv, ACI Mater. J. 88, 240 (1991).
16. T. Hasegawa, T. Shioya and T. Okada, Size effect on splitting tensile strength of concrete. Proceedings of the Japan Concrete Institute 7th Conference, June 1985, pp. 309–312.
17. T. Tang, S.P. Shah and C. Ouyang, J. Struct. Engrg. 118, 3169 (1992).
18. A.M. Neville, Properties of Concrete, fourth edition, Longman, England, 1995.